TECHNICAL NOTES

NATIONAL ADVISORY COMMITTEE FOR AERONAUTICS

No. 506

EXPERIMENTAL VERIFICATION OF THEODORSEN'S THEORETICAL JET-BOUNDARY CORRECTION FACTORS

By George Van Schliestett
Daniel Guggenheim School of Aeronautics
Georgia School of Technology

Washington
October 1934

NATIONAL ADVISORY COMMITTEE FOR AERONAUTICS

TECHNICAL NOTE NO. 506

EXPERIMENTAL VERIFICATION OF THEODORSEN'S THEORETICAL JET-BOUNDARY CORRECTION FACTORS

By George Van Schliestett

SUMMARY

Prandtl's suggested use of a doubly infinite arrangement of airfoil images in the theoretical determination of wind-tunnel jet-boundary corrections was first adapted by Glauert to the case of closed rectangular jets. More recently, Theodorsen, using the same image arrangement but a different analytical treatment, has extended this work to include not only closed but also partly closed and open tunnels.

This report presents the results of wind-tunnel tests conducted at the Georgia School of Technology for the purpose of verifying the five cases analyzed by Theodorsen. The tests were conducted in a square tunnel and the results constitute a satisfactory verification of his general method of analysis. During the preparation of the data two minor errors were discovered in the theory and these have been rectified.

INTRODUCTION

The primary study of wind-tunnel wall interference for circular tunnels was carried out by Prandtl at Göttingen University in 1919. In his paper "Applications of Modern Hydrodynamics to Aeronautics" (reference 1) he points out that owing to the limited cross-sectional area of the wind-tunnel air stream, the deflection of the air behind a model lifting surface is larger or smaller than it would be in free air depending on whether the boundary is open or closed, respectively. To account for this deflection, or downwash, Prandtl demonstrated that it was possible to reproduce theoretically the jet-boundary condition at the test section with the airfoil model in place. To accomplish this result he assumed that the tip vortices of the finite airfoil model were equivalent to a doublet at the

center of the test section, this assumption being justified for span-tunnel width ratios up to 75 percent. Then, to reproduce the circular jet-boundary condition he introduced two imaginary vortices (fig. 1) external to the jet and in the plane of the airfoil doublet, symmetrically spaced at such a distance from the jet center and having such a strength as to provide the appropriate boundary condition. For the open jet, the boundary condition is that of zero normal pressure and for the closed jet, zero normal velocity. The problem is resolved into determining the velocity at the center of the tunnel induced by the imaginary vortices. For the closed tunnel this velocity was found to be:

$$w = \frac{C_L \, S \, V}{8 \, \pi \, R^2}$$

Hence the upward inclination of the air stream due to the interference of the boundary is

$$\epsilon_1 = \frac{w}{V} = \frac{1}{8} \frac{S}{C} C_L$$

where $C = \pi R^2$, R being the radius of the jet. Thus the corrections take the form

$$\Delta \alpha = \delta \frac{S}{C} C_L$$

$$\Delta C_D = \delta \frac{S}{C} C_L^2$$

in which the correction factors are

$\delta = 0.125$ for the closed circular tunnel.

$\delta = -0.125$ for the open circular tunnel.

Prandtl also suggested at this time that for a jet of rectangular cross section "the calculation would have to be made in such a manner that the airfoil was mirrored at all the walls an infinite number of times, like a checkerboard." Working along these lines in 1923, H. Glauert, of Trinity College, Cambridge, contributed his development of the theory for the interference of closed rectangular tunnels (reference 2).

In 1931, Theodorsen of the National Advisory Committee for Aeronautics published the results of an analysis of rectangular-jet corrections covering not only the open and closed cases but also certain forms of partly open and closed jets (fig. 2 and reference 3). His method of summation of the induced velocities differed from that used by Glauert but his numerical results for the closed tunnel were the same.

Glauert in 1932 presented an interpretation (reference 4) of the more accurate formulas developed by Rosenhead in 1930 (reference 5) but confined his discussion to the square and "duplex" closed tunnels, and shortly thereafter published a general theorem on the subject (reference 6) which was as follows: "The interference on very small aerofoils in an open tunnel of any shape is of the same magnitude but opposite in sign as that on the same aerofoil, rotated through a right angle, in a closed tunnel of the same shape."

Early in 1933 Theodorsen presented a study (reference 7) which took into consideration the actual span of the airfoil for the case of the open rectangular jet. A month later a paper by Rosenhead (reference 8), communicated by Glauert, appeared, in which Theodorsen's first monograph (reference 3) was discussed and a different treatment of the subject was presented. Rosenhead's result for Case IV, i.e., vertical boundaries only, disagreed with that of Theodorsen. In this paper Rosenhead quotes a still more general theorem by Glauert to the effect that "The interference on a very small aerofoil in a tunnel, whose boundaries are partly rigid walls and partly free surfaces, is of the same magnitude but opposite in sign, as that on the same aerofoil rotated through a right angle in a tunnel of the same shape as the previous one but where rigid walls replace free surfaces, and free surfaces replace rigid walls."

The present report covers exclusively* the results of airfoil tests made in a square jet with all five of Theodorsen's boundary conditions reproduced for the purpose of verifying his original theoretical analysis in so far as this could be done using a jet of only one shape. The five jet boundaries were as follows:

---

*An experimental investigation on a much broader scale has meanwhile been carried on at Langley Field and the results have been published. (See reference 9.)

Case I - Closed tunnel.

Case II - Free jet.

Case III - Horizontal boundaries.

Case IV - Vertical boundaries.

Case V - One horizontal boundary.

The author wishes to acknowledge the assistance of Professor Montgomery Knight who suggested the investigation and made helpful comments and criticisms, and Professor W. B. Johns to whom thanks are due for his assistance in the analysis of the corrections for Cases IV and V.

METHOD OF TEST

Force tests were made with all five boundary arrangements on a 3 by 18 inch airfoil model (span 60 percent of tunnel width) at a Reynolds Number of 159,000. In addition, a 3 by 12 inch model (span 40 percent of tunnel width) was tested for Cases I and II to observe the effect of span. The basic tunnel had a $2\frac{1}{2}$ foot square open jet (fig. 3). Horizontal pitot-static surveys made with each boundary set-up showed that the maximum variation in dynamic pressure was within 1 percent over the region occupied by the wings.

The forces were measured by means of the wire-balance system shown in figure 4. The lift was measured directly on the large balance as the sum of the forces in the two vertical lift wires. The drag was applied to a horizontal wire, running upstream along the center line of the tunnel, from which the force was transmitted to the vertical wire attached to the drag balance. The forces on the horizontal and vertical wires were equalized by a 45° wire at their juncture. Three lateral wires to the right restrained the cross-wind motion of the model, and a fourth skew wire running downward to the rear and toward the left was attached to a counterweight to hold all wires taut. The various boundaries were set up by bolting plywood walls around the jet as illustrated in figure 4, which shows the closed-jet arrangement.

The two airfoils, 3 by 18 inches and 3 by 12 inches, were made from a single 30-inch blank of laminated mahogany, shaped to a Clark Y section with an initial tolerance of ±0.003 inch in profile. After forming the profile, this long airfoil was cut into the two lengths. The large wing had a fairly uniform twist of 0.5°, producing an error in the correction factor δ_D amounting to 0.041 at $C_L = 0.1$, but rapidly decreasing to 0.002 at $C_L = 0.6$. A twist of 0.3° in the smaller wing caused errors of 0.021 at $C_L = 0.1$ and 0.001 at $C_L = 0.6$. However, these errors had a negligible effect on the results since correction factors near zero lift were not included in the average.

As to precision of measurement, unusual care was observed in reading the balances, since the results depended on the accuracy of determining small differences between relatively large quantities. In order to reduce the possibility of errors due to the changing of static tare, this reading was checked before and after each run. Further accuracy was obtained by making two runs for each set-up. The upward inclination of the air stream ($\epsilon = 0.4°$) was accounted for by making all tests in both the normal and inverted positions and averaging the results.

It was found that the dynamic tare of the frame and wires varied with the angle of attack of the airfoil (figures 5 and 6). This tare was determined by means of a dummy wing in the same position relative to the frame as the real wing, but independently mounted. The dummy wing was moved through the same angle-of-attack range as the test wing and the tare of the frame and wires was thus obtained.

The over-all error of the force measurements was in no case greater than 2 percent and most of the readings were accurate to within 1 percent.

RESULTS

The following equations were used in reducing the test data to coefficient form:

$$C_L = \frac{L}{qS}$$

$$C_{D'} = \frac{D'}{qS}$$

$$\alpha' = \alpha_g - \alpha_{L_o}$$

The symbols used in presenting the results are as follows:

C_L, absolute lift coefficient.

$C_{D'}$, absolute drag coefficient with preliminary corrections, not including jet-boundary effect.

C_D, absolute drag coefficient corrected for jet-boundary effect.

α', angle of attack, in degrees, measured from zero lift.

α, angle of attack measured from zero lift and corrected for jet-boundary effect.

α_g, geometric angle of attack measured with respect to the chord line.

α_{L_o}, geometric angle of attack of zero lift.

L, measured lift.

D', measured drag with preliminary corrections, not including jet-boundary effect.

q, mean dynamic pressure over span of model.

S, area of airfoil.

Although the dynamic-pressure variation in the region occupied by the model was in all cases less than 1 percent, the mean value was found by integrating dynamic pressure readings observed at intervals across the airfoil span for each jet type. The coefficients were calculated on the basis of the mean value. These are presented in nondimensional form in tables I to VII and figures 7 and 8.

The average drag coefficients at zero lift were found to be 0.0239 and 0.0259 for aspect ratios 6 and 4 respectively. The several drag curves were then adjusted so that all had the same minimum drag coefficient corresponding to the foregoing values for the respective aspect ratios as shown in figure 7. The curves of lift against angle of attack were similarly adjusted so that each would pass through $\alpha = 0$ at $C_L = 0$, as shown in figure 8. The effects of turbulence and blocking were not considered in these tests.

The results given in this report are net quantities, the tare of the frame and wires having been subtracted.

The next step was the application of the theoretical jet-boundary corrections. These are of the form:

$$\Delta\alpha = \delta \frac{S}{C} C_L \quad \text{(in radians)}$$

$$= \delta \frac{S}{C} C_L \frac{180}{\pi} \quad \text{(in degrees)}$$

$$\Delta C_D = \delta \frac{S}{C} C_L^2$$

where C is the cross-sectional area of the jet,

and δ is the correction factor from table VIII.

The drag curves first obtained after application of the theoretical correction factors showed Cases IV and V to have large divergences from the other cases as may be seen in figures 9 and 10. The test method was checked, but no possibilities for such large errors could be found. The theory was studied again and analyzed with a view to accounting for these discrepancies. The sources of the errors were discovered and eliminated as described later in the discussion. The new factors were applied to get the correct drag and angle of attack values, which are presented in tables I to VII and figures 9, 10, and 11.

The drag for Case III diverged slightly from the others, but no error in the theory could be found. This matter is discussed later.

The results of the test with one horizontal boundary above the jet and the test with one horizontal boundary below differ from the theoretical results by approximately the same amount but in opposite directions, making the average virtually correct. This average is considered to represent Case V. (See fig. 10.)

Free-air conditions were assumed to be represented by the average corrected results of Cases I, II, IV, and V. (See figs. 9 and 10.)

The experimental correction factors were then calculated from the equations:

$$\delta_D = \frac{\Delta C_D}{\frac{S}{C} C_L^2}$$

$$\delta_\alpha = \frac{\Delta \alpha}{\frac{S}{C} C_L \frac{180}{\pi}}$$

where δ_D is the correction factor for drag

δ_α, correction factor angle of attack

ΔC_D, difference between free air drag and actual test drag at the same lift coefficient

$\Delta \alpha$, difference between free-air angle of attack and actual test angle of attack at the same lift coefficient

Both the theoretical and experimental drag and angle-of-attack corrections are plotted against lift coefficient in figures 12 through 23. From these figures the experimental values of δ for drag and angle of attack were computed for several lift coefficients and listed in tables IX to XV. The average drag and angle-of-attack factors for each jet type were obtained from these tables and are recorded in tables XVI to XX.

ANALYSIS OF DATA

As previously mentioned, when the correction factors were applied to the net force test data large discrepancies were found for Cases IV and V. A thorough analysis of Theodorsen's derivations revealed that in Case IV an effect of appreciable magnitude had been omitted and that in Case V an arithmetical error was present.

In Case IV of his report (reference 3) the line on page 7 beginning "the entire effect ....." should read: the entire effect of all vertical rows of positive doublets extending from $x = mb$ to infinity is thus represented by the effect of a positive vortex row of strength $\frac{\Gamma \Delta L}{b}$ located at $x = (p + \frac{1}{2})\, b$, where p is the number of the last doublet taken into account, and a negative vortex row of the same strength at $x = \text{infinity}$. Then in table I of reference 3:

$$\delta_4 = \frac{\pi}{4} r \left(\sum_1^p \frac{1}{\sinh^2 m \pi r} - \frac{1}{6} \right) + \frac{1}{4} \coth \left(p + \frac{1}{2} \right) \pi r$$

should be

$$\delta_4 = \frac{\pi}{4} r \left(\sum_1^p \frac{1}{\sinh^2 m \pi r} - \frac{1}{6} \right) + \frac{1}{4} \coth \left(p + \frac{1}{2} \right) \pi r - \frac{1}{4} \coth \infty$$

$$= \frac{\pi}{4} r \left(\sum_1^p \frac{1}{\sinh^2 m \pi r} - \frac{1}{6} \right) + \frac{1}{4} \coth \left(p + \frac{1}{2} \right) \pi r - 0.250$$

Correct values of δ_4 obtained by subtracting 0.250 are tabulated in table XXI.

Since the series converges rapidly, the correction factor may also be found for various width-height ratios ≤ 1 from

$$\delta_4 = \frac{\pi}{4} r \left(\sum_1^\infty \frac{1}{\sinh^2 m \pi r} - \frac{1}{6} \right)$$

Values of δ_4 computed from either of the above equations agree with the results obtained by Von Karman with whom the writer has recently corresponded. These results

for Case IV are given in table XXI. It would thus appear that both Theodorsen's and Rosenhead's values for this boundary condition are incorrect, particularly since the ~~wind~~ wind-tunnel tests agree with the corrected theoretical values as shown in table XIX. Moreover, Glauert's later general theorem must be called in question because it does not hold for this case.

In Case V there is an arithmetical error in transferring from

$$v_T = \frac{\Gamma \Delta L}{2\pi} \left(\frac{\pi}{2h}\right)^2 \left[\frac{1}{12} + S_3'\right]$$

$$\delta_5 = \frac{\pi}{4}\frac{r}{2}\left(\sum_1^\infty \frac{(-1)^n \cosh \frac{m\pi r}{2}}{\sinh^2 \frac{m\pi r}{2}} + \frac{1}{12}\right)$$

This should be

$$\delta_5 = \frac{\pi}{16} r \left(\sum_1^\infty \frac{(-1)^n \cosh \frac{m\pi r}{2}}{\sinh^2 \frac{m\pi r}{2}} + \frac{1}{12}\right)$$

The corrected factors, which are one half the magnitude of those in table I of reference 3, are given in table XXI of this report. In this instance, the writer's results are verified by both Von Karman and Rosenhead.

Referring to figures 9 to 11, we find that the drag and angle of attack corrected for jet-boundary effect are equal to free-air drag and angle of attack ±2 percent maximum, except in Case III, which is as much as 3 percent too high. It has been mentioned earlier in this report that Case III does not show close agreement between theory and experiment. Theory gives $\delta = 0.000$ but experiment gives $\delta_D = -0.021$ and $\delta_\alpha = -0.069$ (table XVIII).

It is interesting to note the general similarity in the shape of C_L against ΔC_D and C_L against $\Delta\alpha$ curves for all cases (figs. 12 to 23). Divergence of the experimental curves from those of the theory might possibly be explained by the variable interference effect of the model-supporting frame upon the airfoil.

Tables XVI through XX show satisfactory agreement between experimental and theoretical values of δ with the exception of Case III, as previously mentioned. The various theoretical correction factors for all five cases modified in accordance with the foregoing discussion are listed in table XXI and are plotted against jet width-height ratio b/h, in figure 2. The incorrect curves of both Theodorsen and Rosenhead are included in this figure in the form of broken lines.

CONCLUSIONS

On the basis of these tests the following conclusions may be made:

1. Theodorsen's analytical treatment of the image systems in determining theoretical jet-boundary corrections for square tunnels is satisfactory for ratios of span to tunnel width up to 0.60, the maximum used in these tests.

2. The tests showed that Theodorsen's corrections for Cases IV and V were in error. The values determined as a result of this investigation are for the square tunnel $\delta_4 = -0.126$ and $\delta_5 = -0.063$.

3. After application of the boundary-interference factors, corrected in Cases IV and V, the lift against drag and lift against angle-of-attack curves are equivalent to free-air conditions within ±2 percent, except in Case III, which is 3 percent too large.

4. Theory gives $\delta_3 = 0.000$, but experiment gives $\delta_D = -0.021$ and $\delta_\alpha = -0.069$, for Case III.

5. A single jet boundary above an airfoil does not produce the same interference as a boundary below. The experimental average of the two conditions, however, agrees with the theory.

Daniel Guggenheim School of Aeronautics,
Georgia School of Technology,
Atlanta, Ga., June 20, 1934.

REFERENCES AND BIBLIOGRAPHY

1. Prandtl, L.: Application of Modern Hydrodynamics to Aeronautics. T.R. No. 116, N.A.C.A., 1921.

2. Glauert, H.: The Elements of Aerofoil and Airscrew Theory. Ch. XIV, 1930. Cambridge University Press.

3. Theodorsen, Theodore: The Theory of Wind-Tunnel Wall Interference. T.R. No. 410, N.A.C.A., 1931.

4. Glauert, H.: The Interference on the Characteristics of an Aerofoil in a Wind Tunnel of Rectangular Section. R. & M. No. 1459, British A.R.C., 1932.

5. Rosenhead, L.: The Effect of Wind Tunnel Interference on the Characteristics of an Aerofoil. Royal Society of London Proceedings, (A) 129, 1930, p. 135.

6. Glauert, H.: Some General Theorems Concerning Wind Tunnel Interference on Aerofoils. R. & M. No. 1470, British A.R.C., 1932.

7. Theodorsen, Theodore: Interference on an Airfoil of Finite Span in an Open Rectangular Wind Tunnel. T.R. No. 461, N.A.C.A., 1933.

8. Rosenhead, L.: Interference Due to Walls of a Wind Tunnel. Royal Society of London Proceedings, October-November 1933, pp. 308-320.

9. Theodorsen, Theodore, and Silverstein, Abe: Experimental Verification of the Theory of Wind-Tunnel Boundary Interference. T.R. No. 478, N.A.C.A., 1934.

Knight, Montgomery, and Harris, Thomas A.: Experimental Determination of Jet Boundary Corrections for Airfoil Tests in Four Open Wind Tunnel Jets of Different Shapes. T.R. No. 361, N.A.C.A., 1930.

Higgins, George J.: Wall Interference in Closed Type Wind Tunnels. T.R. No. 256, N.A.C.A., 1927.

Higgins, George J.: The Effect of the Walls in Closed Type Wind Tunnels. T.R. No. 275, N.A.C.A., 1927.

Glauert, H.: The Interference on the Characteristics of an Aerofoil in a Wind Tunnel of Circular Section. R. & M. No. 1453, British A.R.C., 1932.

TABLE I. FORCE TEST

Case I - Closed tunnel

Clark Y airfoil 3 by 18 inches

C_L	C_D'	$*\Delta C_D$	C_D	α'	$*\Delta\alpha$	α
0	0.0239	0.0000	0.0239	0	0	0
.094	.0219	.0001	.0220	1.05	.04	1.09
.188	.0212	.0003	.0215	2.10	.09	2.19
.375	.0235	.0012	.0247	4.25	.17	4.42
.563	.0316	.0026	.0342	6.45	.26	6.71
.751	.0441	.0046	.0487	8.75	.35	9.10
.938	.0604	.0072	.0676	11.15	.44	11.59
1.127	.0817	.0104	.0921	13.75	.53	14.28
1.221	.0956	.0121	.1077	15.25	.57	15.82

*Theoretical corrections.

TABLE II. FORCE TEST

Case I - Closed tunnel

Clark Y airfoil 3 by 12 inches

C_L	C_D'	$*\Delta C_D$	C_D	α'	$*\Delta\alpha$	α
0	0.0259	0.0000	0.0259		0	0
.141	.0244	.0001	.0245	1.95	.04	1.99
.282	.0265	.0004	.0269	3.85	.09	3.94
.422	.0329	.0010	.0339	5.80	.13	5.93
.563	.0438	.0017	.0455	7.80	.18	7.98
.704	.0579	.0027	.0606	9.85	.22	10.07
.845	.0752	.0039	.0791	11.95	.26	12.21
.986	.0959	.0053	.1012	14.10	.31	14.41
1.127	.1218	.0069	.1287	16.35	.35	16.70

*Theoretical corrections.

TABLE III. FORCE TEST

Case II - Free jet

Clark Y airfoil 3 by 18 inches

C_L	C_D'	$*\Delta C_D$	C_D	α'	$*\Delta\alpha$	α
0	0.0239	0.0000	0.0239	0	0	0
.094	.0220	-.0001	.0219	1.15	-.04	1.11
.188	.0217	-.0003	.0214	2.25	-.09	2.16
.375	.0257	-.0011	.0246	4.55	-.17	4.38
.563	.0356	-.0026	.0330	6.95	-.26	6.69
.751	.0512	-.0046	.0466	9.40	-.35	9.05
.938	.0733	-.0072	.0661	12.00	-.44	11.56
1.127	.1016	-.0103	.0913	14.75	-.53	14.22
1.221	.1185	-.0121	.1064	16.25	-.57	15.68

*Theoretical corrections.

TABLE IV. FORCE TEST

Case II - Free jet

Clark Y airfoil 3 by 12 inches

C_L	C_D'	$*\Delta C_D$	C_D	α'	$*\Delta\alpha$	α
0	0.0259	0.0000	0.0259	0	0	0
.141	.0248	-.0001	.0247	2.00	-.04	1.96
.282	.0277	-.0004	.0273	4.05	-.09	3.96
.422	.0354	-.0010	.0344	6.10	-.13	5.97
.563	.0468	-.0017	.0451	8.20	-.18	8.02
.704	.0625	-.0027	.0598	10.30	-.22	10.08
.845	.0827	-.0039	.0788	12.45	-.26	12.19
.986	.1069	-.0053	.1016	14.65	-.31	14.34
1.127	.1356	-.0069	.1287	17.00	-.35	16.65

*Theoretical corrections.

TABLE V. FORCE TEST

Case III - Horizontal boundaries

Clark Y airfoil 3 by 18 inches

C_L	C_D'	$*\Delta C_D$	C_D	α'	$*\Delta\alpha$	α
0	0.0239	0.000	0.0239	0	0.00	0
.094	.0223	.000	.0223	1.10	.00	1.10
.188	.0219	.000	.0219	2.20	.00	2.20
.375	.0253	.000	.0253	4.50	.00	4.50
.563	.0338	.000	.0338	6.85	.00	6.85
.751	.0481	.000	.0481	9.25	.00	9.25
.938	.0681	.000	.0681	11.85	.00	11.85
1.127	.0938	.000	.0938	14.65	.00	14.65
1.221	.1097	.000	.1097	16.15	.00	16.15

*Theoretical corrections.

TABLE VI. FORCE TEST

Case IV - Vertical boundaries

Clark Y airfoil 3 by 18 inches

C_L	C_D'	$*\Delta C_D$	C_D	α'	$*\Delta\alpha$	α
0	0.0239	0.0000	0.0239	0	0	0
.094	.0222	-.0001	.0221	1.15	-.04	1.11
.188	.0225	-.0003	.0222	2.30	-.08	2.22
.375	.0266	-.0010	.0256	4.60	-.16	4.44
.563	.0359	-.0023	.0336	7.00	-.24	6.76
.751	.0513	-.0042	.0471	9.45	-.32	9.13
.938	.0727	-.0065	.0662	12.05	-.40	11.65
1.127	.0997	-.0094	.0903	14.90	-.48	14.42
1.221	.1152	-.0109	.1043	16.45	-.52	15.93

*Theoretical corrections.

TABLE VII(a). FORCE TEST

Case V - Upper horizontal boundary

Clark Y airfoil 3 by 18 inches

C_L	C_D'	$*\Delta C_D$	C_D	α'	$*\Delta\alpha$	α
0	0.0239	0.0000	0.0239	0	0	0
.094	.0225	.0000	.0225	1.10	-.02	1.08
.188	.0224	-.0001	.0223	2.20	-.04	2.16
.375	.0266	-.0005	.0261	4.50	-.08	4.42
.563	.0362	-.0012	.0350	6.85	-.12	6.73
.751	.0520	-.0021	.0499	9.25	-.16	9.09
.938	.0717	-.0033	.0684	11.75	-.20	11.55
1.127	.0968	-.0048	.0920	14.40	-.24	14.16
1.221	.1135	-.0056	.1079	15.90	-.26	15.64

*Theoretical corrections.

TABLE VII(b). FORCE TEST

Case V - Lower horizontal boundary

Clark Y airfoil 3 by 18 inches

C_L	C_D'	$*\Delta C_D$	C_D	α'	$*\Delta\alpha$	α
0	0.0239	0.0000	0.0239	0	0	0
.094	.0221	.0000	.0221	1.15	-.02	1.13
.188	.0218	-.0001	.0217	2.25	-.04	2.21
.375	.0251	-.0005	.0246	4.60	-.08	4.52
.563	.0341	-.0012	.0329	6.90	-.12	6.78
.751	.0483	-.0021	.0462	9.35	-.16	9.19
.938	.0682	-.0033	.0649	11.85	-.20	11.65
1.127	.0942	-.0048	.0894	14.60	-.24	14.36
1.221	.1101	-.0056	.1045	16.15	-.26	15.89

*Theoretical corrections.

TABLE VII(c). FORCE TEST

Case V - One horizontal boundary

Average of tables VII(a) and VII(b)

Clark Y airfoil 3 by 18 inches

C_L	C_D'	$*\Delta C_D$	C_D	α'	$*\Delta\alpha$	α
0	0.0239	0.0000	0.0239	0	0	0
.094	.0223	.0000	.0223	1.10	-.02	1.08
.188	.0221	-.0001	.0220	2.20	-.04	2.16
.375	.0259	-.0005	.0254	4.55	-.08	4.47
.563	.0351	-.0012	.0339	6.90	-.12	6.78
.751	.0497	-.0021	.0476	9.30	-.16	9.14
.938	.0695	-.0033	.0662	11.80	-.20	11.60
1.127	.0956	-.0048	.0908	14.50	-.24	14.26
1.221	.1118	-.0056	.1062	16.05	-.26	15.79

*Theoretical corrections.

TABLE VIII. THEORETICAL δ

(Table I in reference 3)

r	δ_1	δ_2	δ_3	δ_4	δ_5
0	∞	$-\infty$	$-\infty$	∞	$-\infty$
.125	1.055	-0.524	-0.524	1.051	-1.050
.25	.523	-.262	-.262	.524	-.524
.50	.263	-.137	-.127	.262	-.262
.625	.213	-.122	-.089	.210	-.208
.75	.175	-.120	-.056	.161	-.173
1.00	.138	-.137	.000	.124	-.127
1.50	.120	-.197	.077	.054	-.056
2.00	.137	-.262	.126	-.012	.000
4.00	.262	-.524	.262	-.276	.126
∞	∞	$-\infty$	∞	$-\infty$	∞

TABLE IX. EXPERIMENTAL δ

Case I - Closed tunnel

Clark Y airfoil 3 by 18 inches

$$\delta_D = \frac{\Delta C_D}{\frac{S}{C} C_L^2} \qquad \delta_\alpha = \frac{\Delta \alpha}{\frac{S}{C} C_L \frac{180}{\pi}}$$

C_L	ΔC_D	δ_D	$\Delta \alpha$	δ_α
0.1	(0.0002)	(0.336)	0.05	0.146
.2	(.0007)	(.293)	.09	.132
.3	(.0013)	(.243)	.14	.137
.4	.0016	.168	.20	.146
.5	.0019	.128	.26	.152
.6	.0023	.109	.30	.146
.7	.0031	.106	.34	.142
.8	.0043	.113	.38	.139
.9	.0058	.121	.43	.140
1.0	.0075	.126	.49	.143
1.1	.0093	.129	.54	.144
1.2	.0108	.126	.56	.137
Average		.125		.142

Quantities in parentheses not averaged because of large discrepancies. ΔC_D from figure 12. $\Delta \alpha$ from figure 19.

TABLE X. EXPERIMENTAL δ

Case I - Closed tunnel

Clark Y airfoil 3 by 12 inches

$$\delta_D = \frac{\Delta C_D}{\frac{S}{C} C_L^2} \qquad \delta_\alpha = \frac{\Delta \alpha}{\frac{S}{C} C_L \frac{180}{\pi}}$$

C_L	ΔC_D	δ_D	$\Delta\alpha$	δ_α
0.1	(0.0001)	(0.252)	(0.02)	(0.088)
.2	(.0003)	(.189)	.06	.132
.3	.0006	.168	.11	.161
.4	.0011	.174	.14	.154
.5	.0014	.142	.18	.158
.6	.0016	.113	.21	.154
.7	.0022	.114	.23	.144
.8	.0032	.126	.24	.132
.9	.0044	.137	.26	.127
1.0	.0057	.144	.27	.119
1.1	.0066	.138	.31	.120
Average		.140		.140

Quantities in parentheses not averaged because of large discrepancies. ΔC_D from figure 13. $\Delta\alpha$ from figure 19.

TABLE XI. EXPERIMENTAL δ

Case II - Free jet

Clark Y airfoil 3 by 18 inches

$$\delta_D = \frac{\Delta C_D}{\frac{S}{C} C_L^2} \qquad \delta_\alpha = \frac{\Delta \alpha}{\frac{S}{C} C_L \frac{180}{\pi}}$$

C_L	ΔC_D	δ_D	$\Delta\alpha$	δ_α
0.1	(0.0003)	(0.503)	(0.05)	(0.142)
.2	.0004	.168	(.07)	(.103)
.3	.0007	.131	(.10)	(.097)
.4	.0012	.126	(.13)	(.095)
.5	.0019	.128	(.18)	(.106)
.6	.0026	.121	.23	.112
.7	.0033	.113	.27	.113
.8	.0044	.116	.32	.117
.9	.0060	.125	.38	.124
1.0	.0082	.138	.43	.126
1.1	.0101	.140	.45	.120
1.2	.0117	.137	.45	.110
Average		-.132		-.117

Quantities in parentheses not averaged because of large discrepancies. ΔC_D from figure 14. $\Delta\alpha$ from figure 20.

TABLE XII. EXPERIMENTAL δ

Case II - Free jet

Clark Y airfoil 3 by 12 inches

$$\delta_D = \frac{\Delta C_D}{\frac{S}{C} C_L^2} \qquad \delta_\alpha = \frac{\Delta \alpha}{\frac{S}{C} C_L \frac{180}{\pi}}$$

C_L	ΔC_D	δ_D	$\Delta\alpha$	δ_α
0.1	(0.0001)	(0.252)	(0.04)	(0.176)
.2	(.0003)	(.189)	.07	.154
.3	(.0007)	(.197)	.08	.117
.4	(.0012)	(.190)	.14	.154
.5	.0014	.142	(.19)	(.167)
.6	.0016	.113	.20	.146
.7	.0023	.119	.22	.138
.8	.0033	.130	.24	.132
.9	.0045	.141	.26	.127
1.0	.0057	.144	.28	.123
1.1	.0066	.138	.31	.124
Average		-.131		-.137

Quantities in parentheses not averaged because of large discrepancies. ΔC_D from figure 15. $\Delta\alpha$ from figure 20.

TABLE XIII. EXPERIMENTAL δ

Case III - Horizontal boundaries

Clark Y airfoil 3 by 18 inches

$$\delta_D = \frac{\Delta C_D}{\frac{S}{C} C_L^2} \qquad \delta_\alpha = \frac{\Delta \alpha}{\frac{S}{C} C_L \frac{180}{\pi}}$$

C_L	ΔC_D	δ_D	$\Delta \alpha$	δ_α
0.1	(0.0002)	(0.336)	(0.00)	(0.000)
.2	(.0001)	(.084)	(.02)	(.029)
.3	.0001	.019	.05	.043
.4	.0002	.042	.08	.059
.5	.0002	.013	.10	.073
.6	.0001	.005	.11	.054
.7	.0002	.007	.13	.054
.8	.0005	.013	.16	.059
.9	.0010	.021	.22	.072
1.0	.0015	.025	.30	.088
1.1	.0021	.029	.35	.093
1.2	.0028	.033	.34	.083
Average		-.021		-.069

Quantities in parentheses not averaged because of large discrepancies. ΔC_D from figure 16. $\Delta \alpha$ from figure 21.

TABLE XIV. EXPERIMENTAL δ

Case IV - Vertical boundaries

Clark Y airfoil 3 by 18 inches

$$\delta_D = \frac{\Delta C_D}{\frac{S}{C} C_L^2} \qquad \delta_\alpha = \frac{\Delta \alpha}{\frac{S}{C} C_L \frac{180}{\pi}}$$

C_L	ΔC_D	δ_D	$\Delta\alpha$	δ_α
0.1	(0.0001)	(0.168)	(0.05)	(0.147)
.2	(.0007)	(.293)	(.12)	(.176)
.3	(.0012)	(.224)	.14	.137
.4	(.0016	(.168)	.18	.132
.5	.0020	.134	.23	.135
.6	.0024	.112	.28	.137
.7	.0030	.103	.32	.134
.8	.0041	.108	.36	.132
.9	.0054	.112	.42	.137
1.0	.0067	.113	.50	.147
1.1	.0086	.111	.58	.155
1.2	(.0085)	(.099)	.61	.149
Average		-.113		-.139

Quantities in parentheses not averaged because of large discrepancies. ΔC_D from figure 17. $\Delta\alpha$ from figure 22.

TABLE XV. EXPERIMENTAL δ

Case V - One horizontal boundary

Clark Y airfoil 3 by 18 inches

$$\delta_D = \frac{\Delta C_D}{\frac{S}{C} C_L^2} \qquad \delta_\alpha = \frac{\Delta \alpha}{\frac{S}{C} C_L \frac{180}{\pi}}$$

C_L	ΔC_D	δ_D	$\Delta\alpha$	δ_α
0.1	(0.0002)	(0.336)	(0.04)	(0.117)
.2	(.0003)	(.126)	(.06)	(.088)
.3	.0005	.093	(.05)	(.049)
.4	.0009	.095	(.04)	(.029)
.5	.0012	.081	(.07)	(.041)
.6	.0016	.075	.09	.044
.7	.0021	.075	.11	.046
.8	.0026	.068	.15	.055
.9	.0030	.062	.18	.059
1.0	.0033	.055	.23	.067
1.1	.0038	.053	.27	.072
1.2	.0048	.056	.28	.068
Average		-.071		-.059

Quantities in parentheses not averaged because of large discrepancies. ΔC_D from figure 18. $\Delta\alpha$ from figure 23.

TABLE XVI. CORRECTION FACTORS

Case I - Square closed tunnel

	3 by 12 inch airfoil		3 by 18 inch airfoil	
	δ_D	δ_α	δ_D	δ_α
Theoretical	0.138	0.138	0.138	0.138
Experimental	.140	.140	.125	.142

TABLE XVII. CORRECTION FACTORS

Case II - Square open jet

	3 by 12 inch airfoil		3 by 18 inch airfoil	
	δ_D	δ_α	δ_D	δ_α
Theoretical	-0.137	-0.137	-0.137	-0.137
Experimental	-.131	-.137	-.132	-.117

TABLE XVIII. CORRECTION FACTORS

Case III - Square jet with horizontal boundaries

3 by 18 inch airfoil

	δ_D	δ_α
Theoretical	0.000	0.000
Experimental	-.021	-.069

TABLE XIX. CORRECTION FACTORS

Case IV - Square jet with vertical boundaries

3 by 18 inch airfoil

	δ_D	δ_α
Theoretical	-0.126	-0.126
Experimental	-.113	-.139

TABLE XX. CORRECTION FACTORS

Case V - Square jet with one horizontal boundary

3 by 18 inch airfoil

	δ_D	δ_α
Theoretical	-0.063	-0.063
Experimental	-.071	-.059

TABLE XXI. THEORETICAL δ

(With δ_4 and δ_5 of table I, reference 3, corrected)

$$\delta_1 = \frac{\pi}{4} r\left(\sum_1^p \frac{\cosh n\pi r}{\sinh^2 n\pi r} + \frac{1}{12}\right) + \frac{1}{4 \sinh(p + \frac{1}{2})\pi r} \text{ closed tunnel}$$

$$\delta_2 = \frac{\pi}{4} r\left(\sum_1^\infty \frac{(-1)^n}{\sinh^2 n\pi r} - \frac{1}{6}\right) \text{free jet}$$

$$\delta_3 = \frac{\pi}{4} r\left(\sum_1^\infty \frac{(-1)^n \cosh n\pi r}{\sinh^2 n\pi r} + \frac{1}{12}\right) \text{horizontal boundaries}$$

$$\delta_4 = \frac{\pi}{4} r\left(\sum_1^p \frac{1}{\sinh^2 n\pi r} - \frac{1}{6}\right) + \frac{1}{4} \coth (p + \tfrac{1}{2}) \pi r - 0.25$$

vertical boundaries

$$\delta_5 = \frac{\pi}{16} r \left(\sum_1^\infty \frac{(-1)^n \cosh \frac{m\pi r}{2}}{\sinh^2 \frac{m\pi r}{2}} + \frac{1}{12}\right) \text{one horizontal boundary}$$

r	δ_1	δ_2	δ_3	δ_4	δ_5
0	∞	$-\infty$	$-\infty$	∞	$-\infty$
.125	1.055	-0.524	-0.524	0.801	-0.525
.250	.523	-.262	-.262	.274	-.262
.50	.263	-.137	-.127	.012	-.131
.625	.213	-.122	-.089	-.040	-.104
.75	.175	-.120	-.056	-.089	-.086
1.00	.138	-.137	.000	-.126	-.063
1.50	.120	-.197	.077	-.196	-.028
2.00	.137	-.262	.126	-.262	.000
4.00	.262	-.524	.262	-.526	.063
∞	∞	$-\infty$	∞	$-\infty$	∞

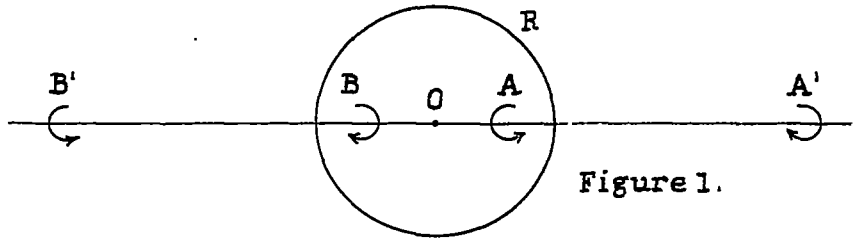

Figure 1.

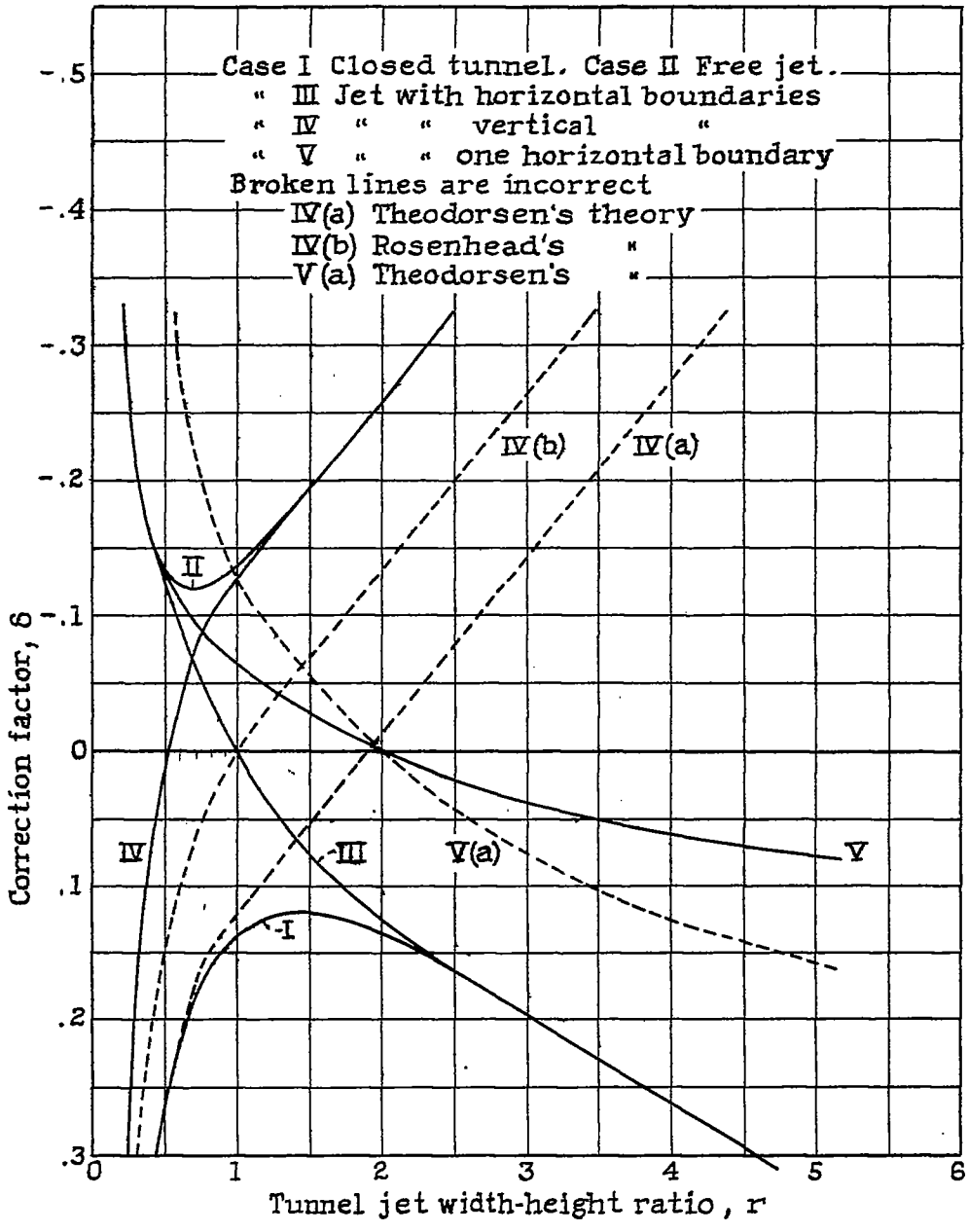

Figure 2.- Tunnel-wall correction, δ

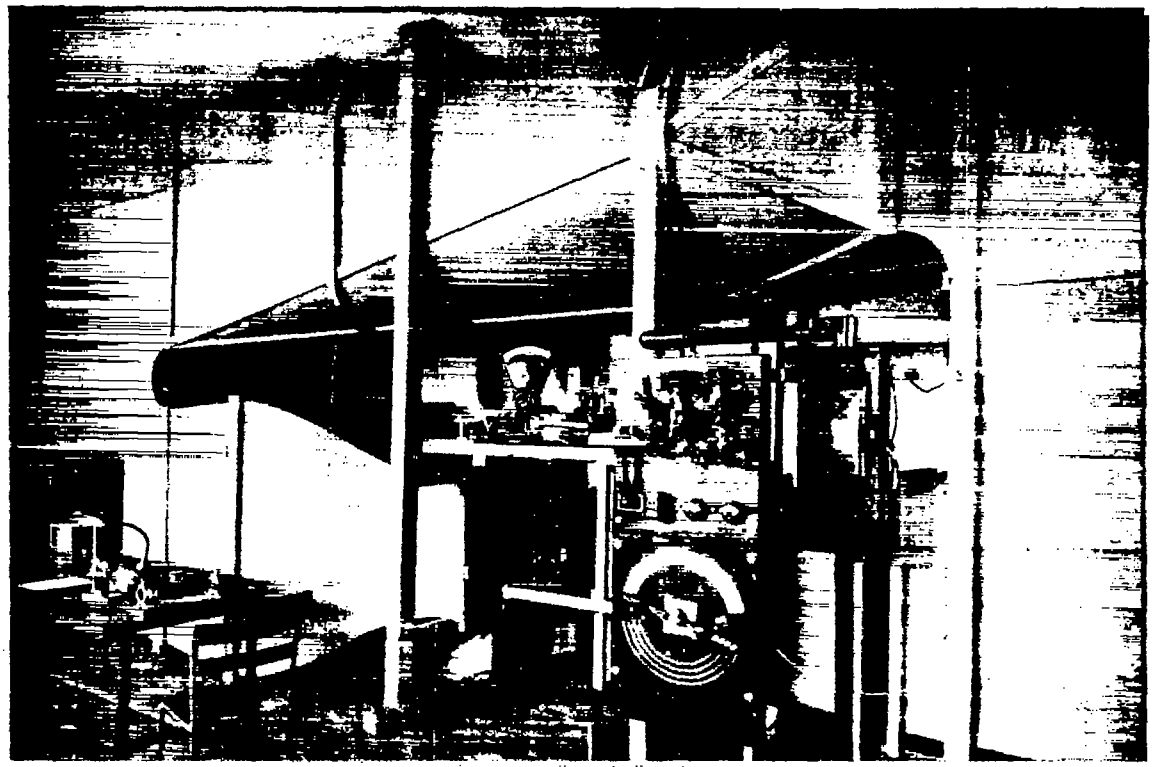

Figure 3.-The 2 1/2 ft. open jet wind tunnel of the Georgia School of Technology.

Figure 4.-The 2 1/2 ft. closed wind tunnel of the Georgia School of Technology.

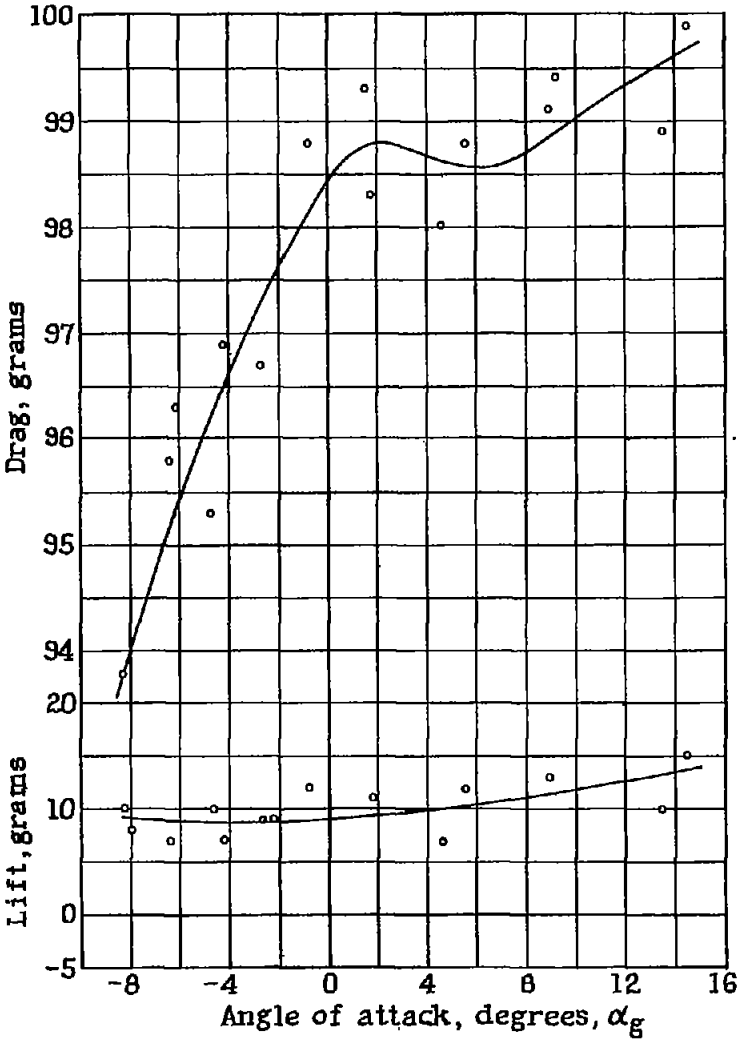

Figure 5.- Dynamic tare forces. Six-component balance frame. Case I. Tunnel closed. Airfoil in normal test position.

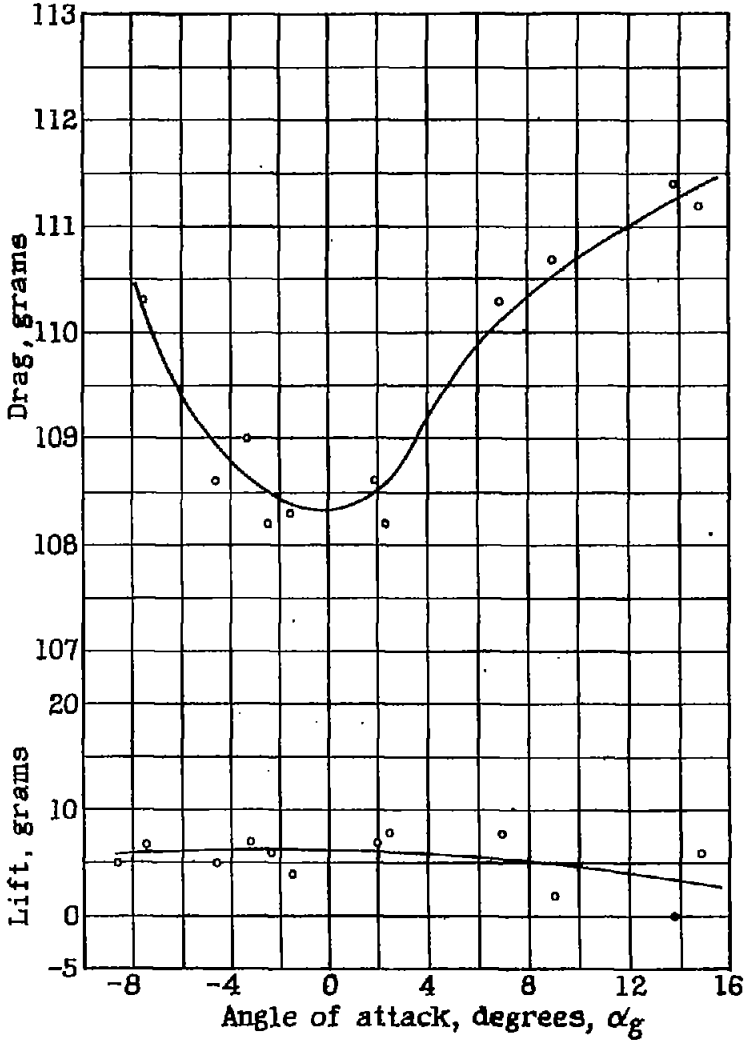

Figure 6.- Dynamic tare forces. Six-component balance frame. Case I. Tunnel closed. Airfoil in inverted test position.

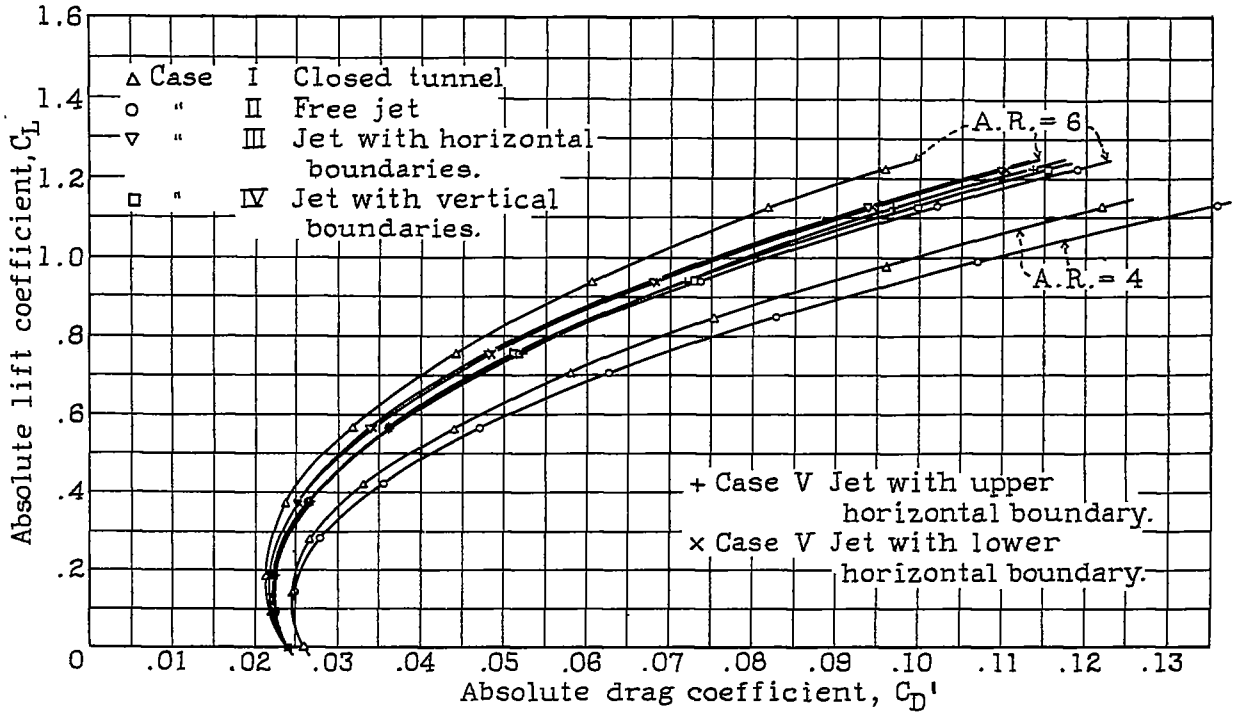

Figure 7. - Lift - drag polars uncorrected for jet - boundary effect.

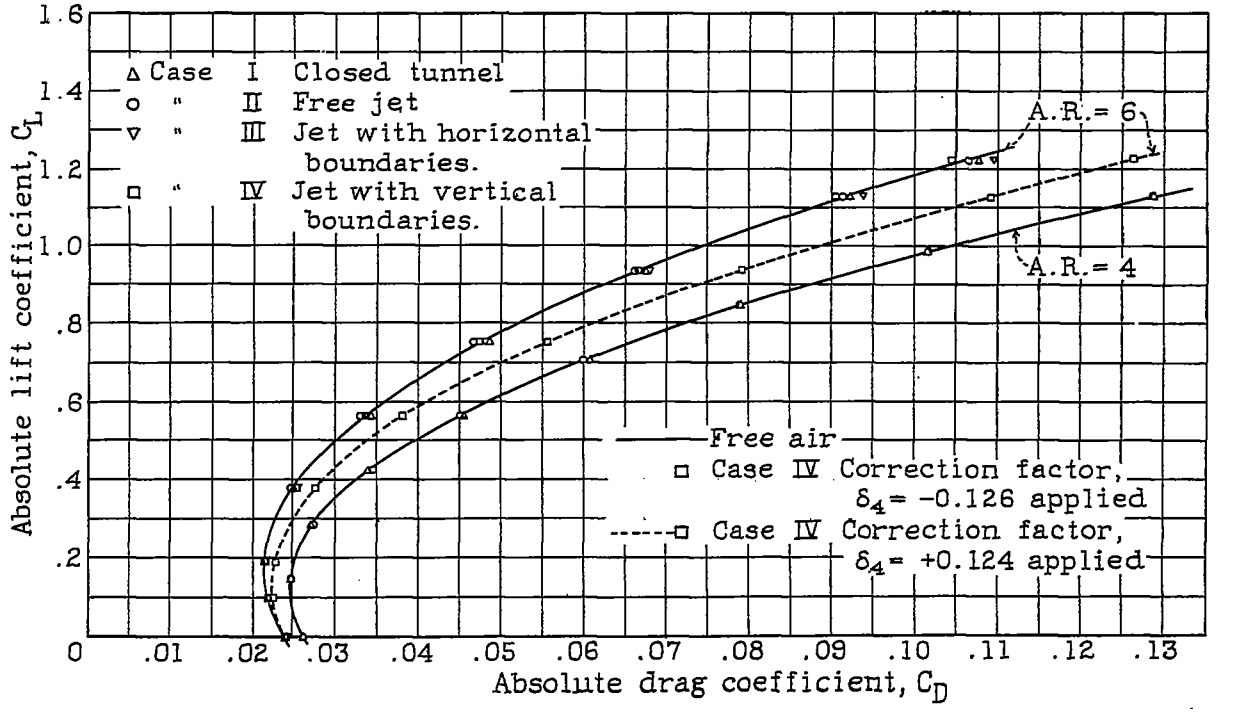

Figure 9. - Lift - drag polars corrected for jet - boundary effect.

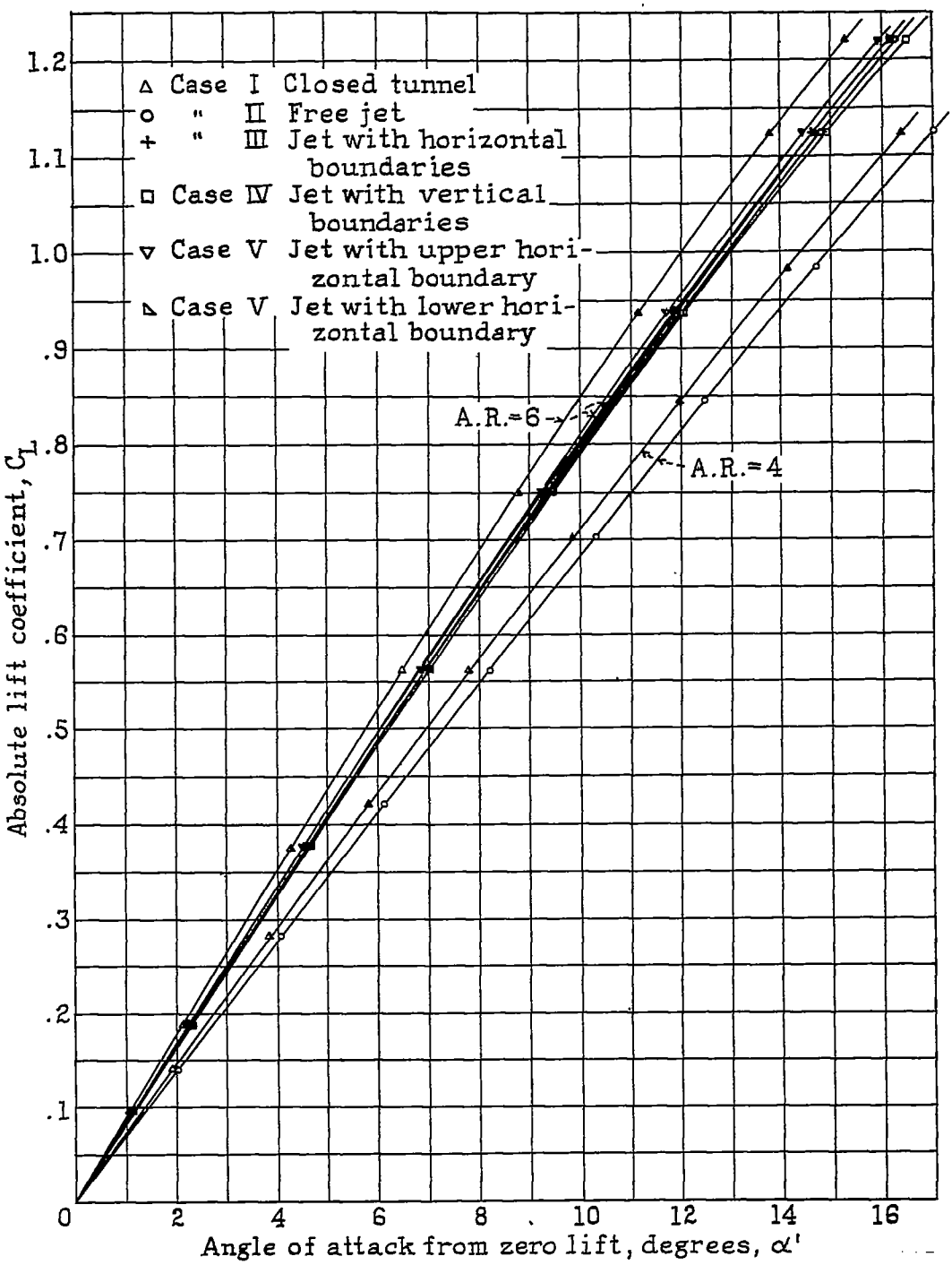

Figure 8.- Lift against angle of attack uncorrected for jet-boundary effect.

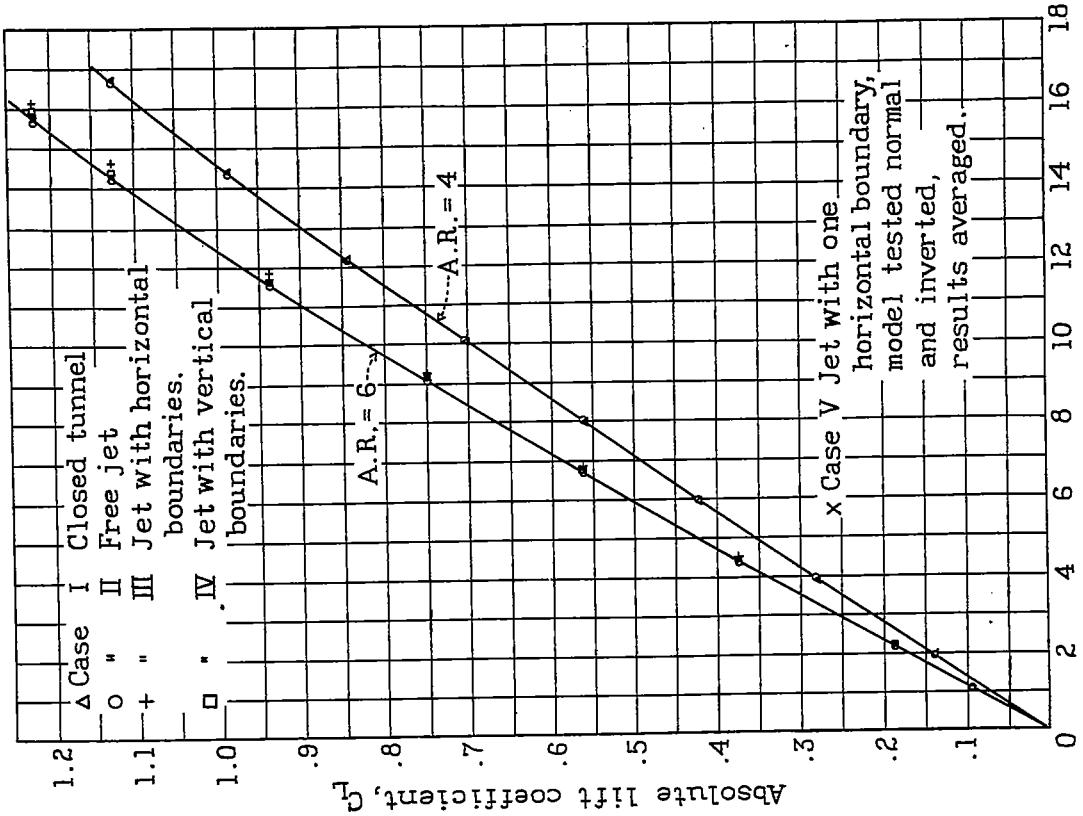

Figure 11.- Lift against angle of attack corrected for jet-boundary effect.

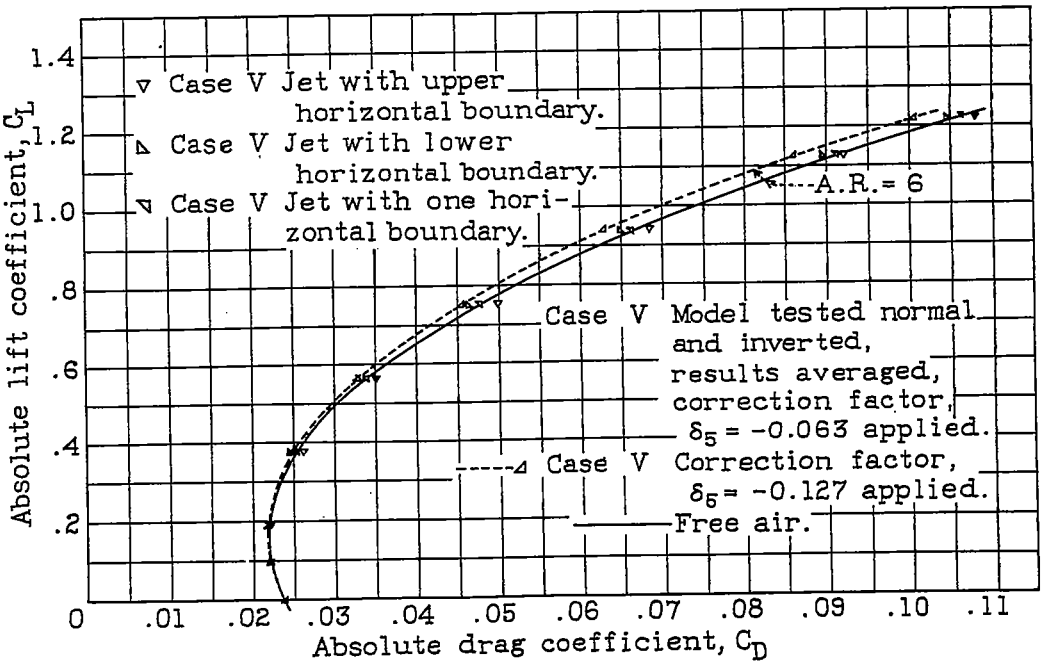

Figure 10. - Lift - drag polars corrected for jet-boundary effect.

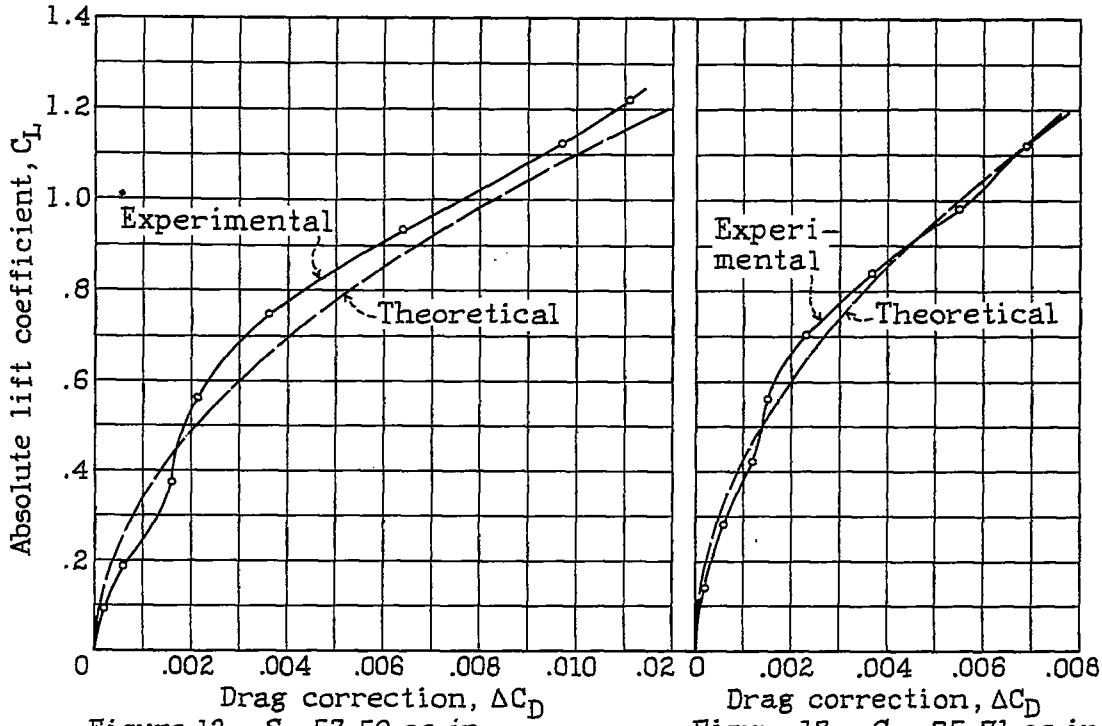

Figure 12.- S = 53.59 sq.in. Clark Y airfoil 3 by 18 inches.

Figure 13.- S = 35.71 sq.in. Clark Y airfoil 3 by 12 inches.

Case I. Tunnel closed. C = 900 sq.in.

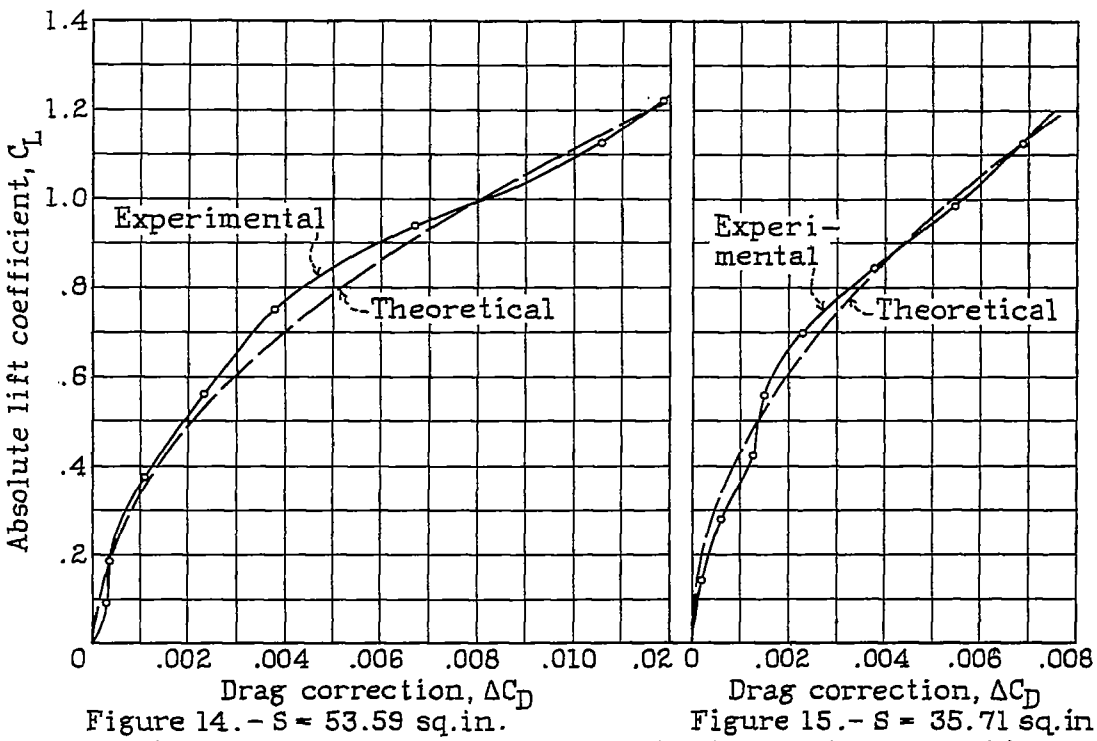

Figure 14.- S = 53.59 sq.in. Clark Y airfoil 3 by 18 inches.

Figure 15.- S = 35.71 sq.in. Clark Y airfoil 3 by 12 inches.

Case II. Free jet. C = 900 sq.in.

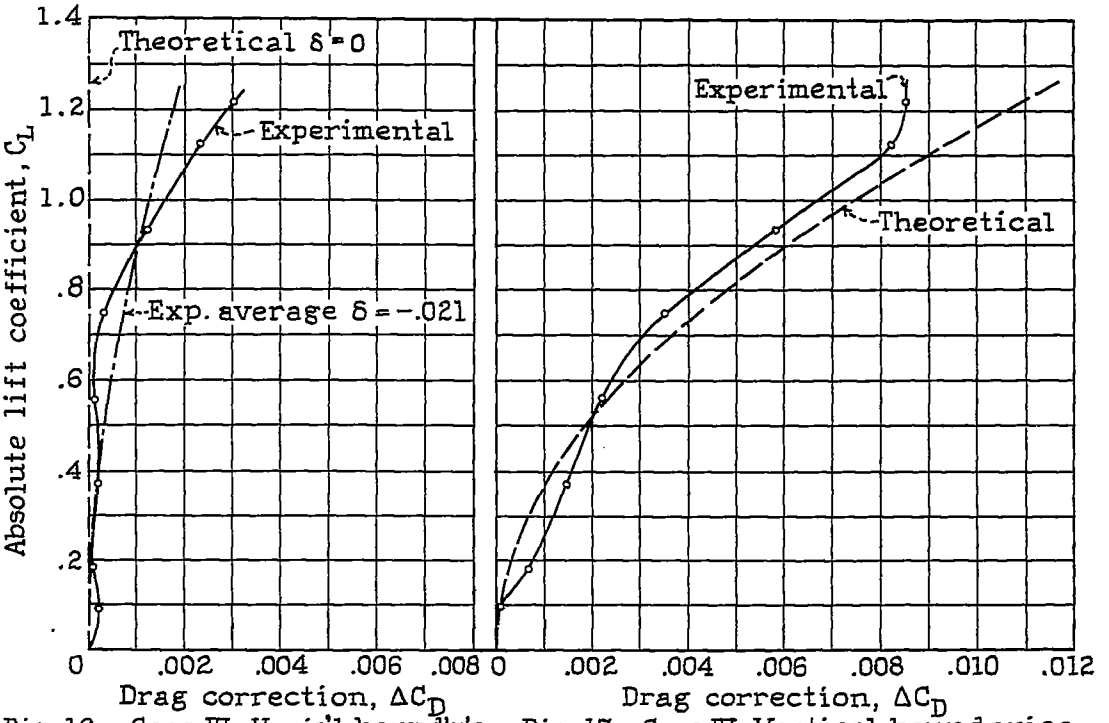

Fig. 16.- Case III. Horiz'l bound'r's. Clark Y airfoil 3 by 18 inches. S = 53.59 sq. in. C = 900 sq. in.

Fig. 17.- Case IV. Vertical boundaries.

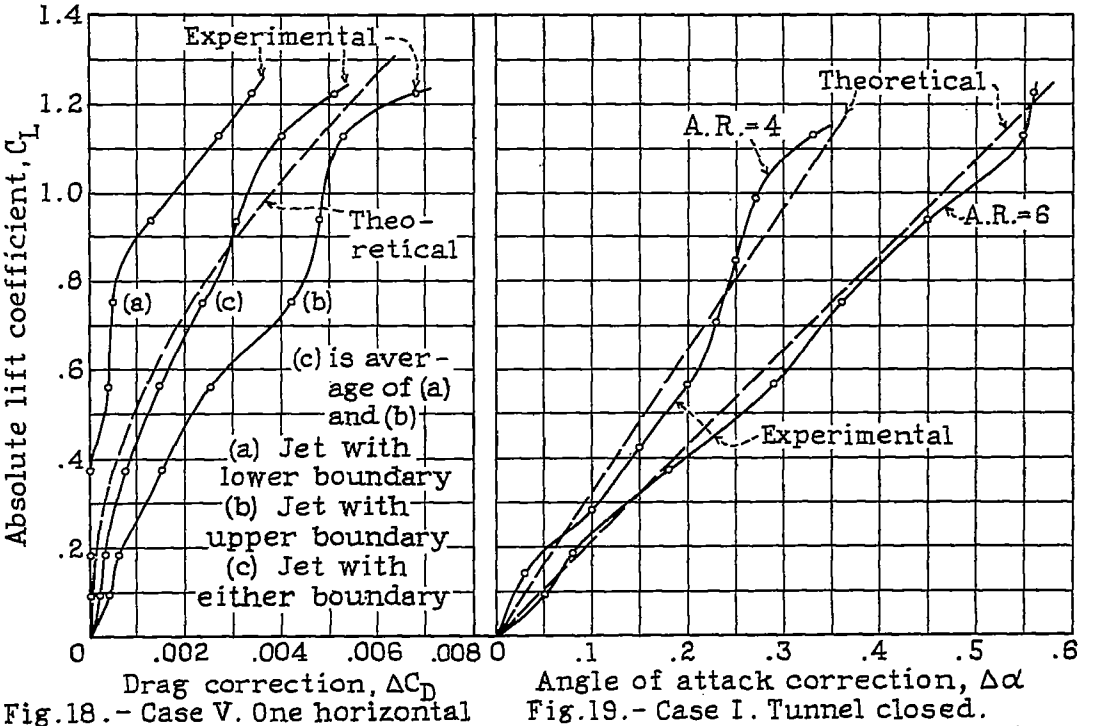

Fig. 18.- Case V. One horizontal boundary. Clark Y airfoil 3" x 18". S = 53.59 sq. in. C = 900 sq. in. Airfoil tested in normal and inverted positions.

Fig. 19.- Case I. Tunnel closed. Clark Y airfoils 3 by 18 in. & 3 by 12 in. S_6 = 53.59 sq. in. and S_4 = 35.71 sq. in. C = 900 sq. in.

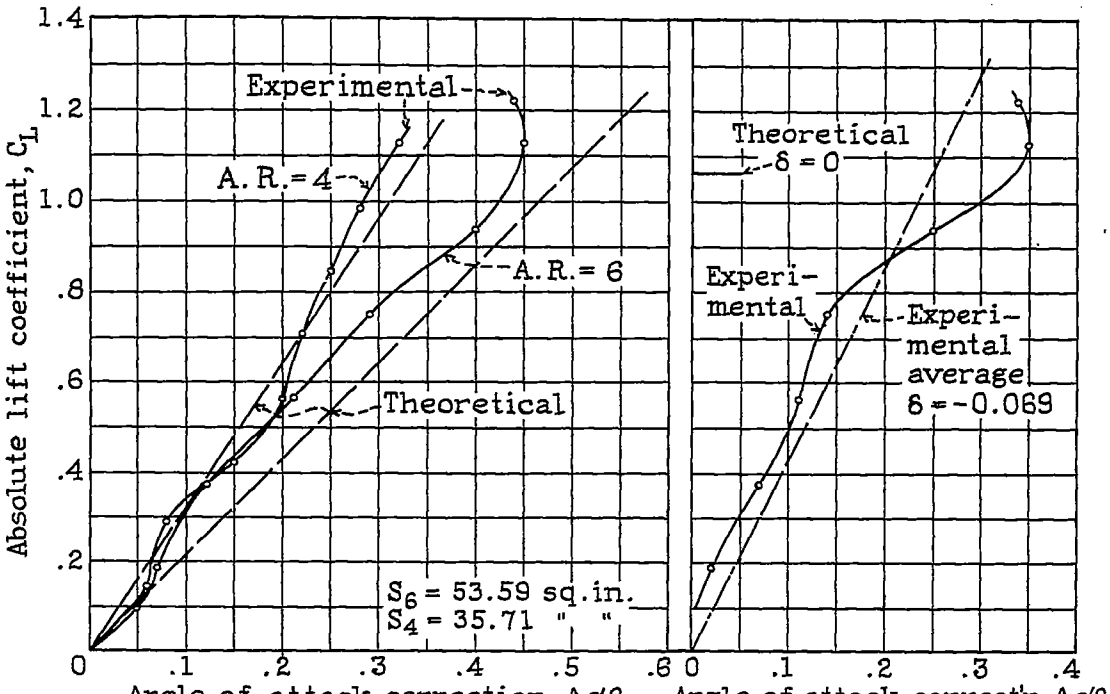

Figure 20.- Case II. Free jet. Clark Y airfoils 3 by 18 in. and 3 by 12 in. C = 900 sq. in.

Fig. 21.- Case III. Horiz'l. boundaries. Clark Y airfoil 3 by 18 in. S = 53.59 sq. in. C = 900 sq. in.

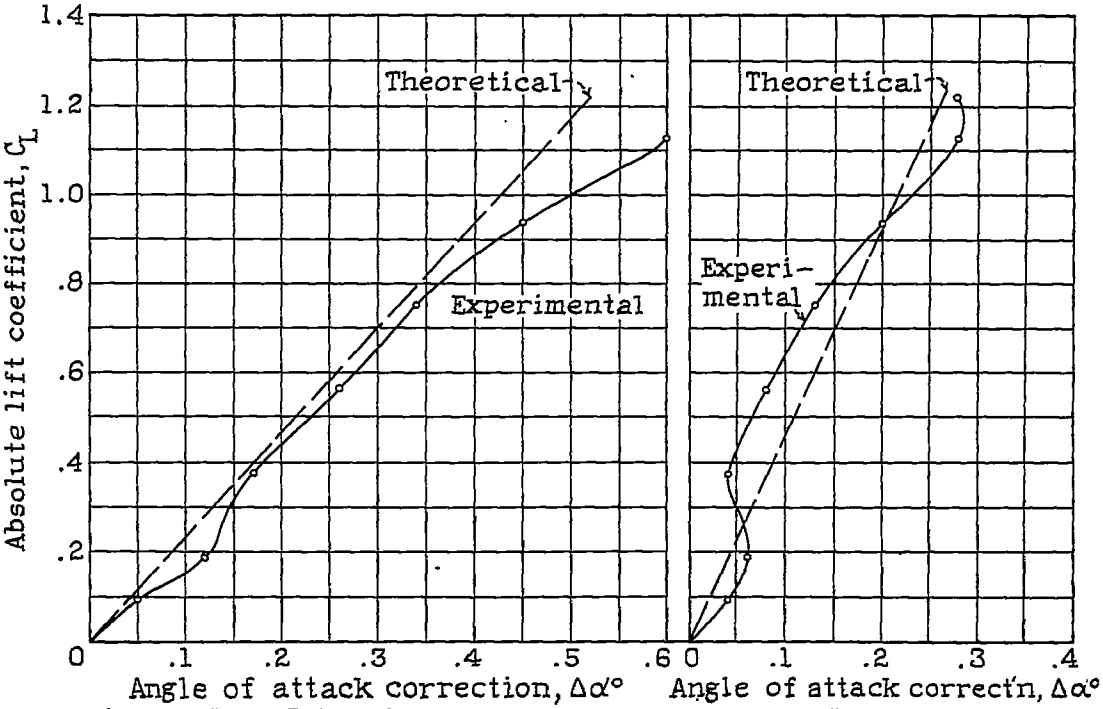

Fig. 22.- Case IV. Vertical boundaries. Clark Y airfoil 3 by 18 inches. S = 53.59 sq. in. C = 900 sq. in.

Fig. 23.- Case V. One horiz'l boundary. Clark Y, 3 by 18 in. S = 53.59 sq. in. C = 900 sq. in.